Preprints of the 21st IFAC World Congress (Virtual)
Berlin, Germany, July 12-17, 2020

Assessment Criteria for the Mechanical Loads of Wind Turbines applied to the example of Active Power Control

Christian Clemens Eckhard Gauterin Florian Pöschke Horst Schulte

University of Applied Sciences (HTW) Berlin,
Department of Engineering I, Control Engineering Group,
Wilhelminenhofstr. 75A 12459 Berlin, Germany,
Email: christian-clemens@gmx.net, schulte@htw-berlin.de

Abstract: Assessment criteria for design of wind turbines controller are discussed since conventional control performance criteria are not sufficient to evaluate the mechanical loads as dependency of the controller type and settings. This will be presented and discussed using the example of the active power control of wind turbines. In contrast to the nominal operation of wind turbines divided into power optimization in the partial and power limitation in the full load region, the power output is guided by an external power reference signal. The reference signal may be delivered either directly by higher-level load frequency controller of the power system or by the wind farm controller. In both cases the external variation of the power to be delivered has an enormous influence on the dynamics and mechanical loads of the wind turbine. To quantify these loads that occur during power tracking operation the Damage Equivalent Load amplitude as appropriated load assessment criteria is described and prepared for control design.

Keywords: Control of renewable energy resources, Damage Equivalent Load, Control system design

1. INTRODUCTION

The design of the mechanical components of wind turbines, like tower, drive train or rotor blades is driven by the mechanical loads occurring within the installation and fully automated operation of the turbine. Therefore, conventional control performance criteria, such as control rise time or maximum overshoot are not sufficient for wind turbine controller design. Industry standards like IEC61400-1 (2005) or DNV-GL (2016) define detailed specifications for the environmental conditions which include the intensity of wind and wave excitation, calculation guidelines as well as analysis of the resulting mechanical loads, i.e. extreme and fatigue loads. To implement those specifications within the controller design process the total and overall Damage Equivalent Load (DEL) is presented in this work as an assessment criteria of the occurring fatigue loads in wind turbine components.

Additional to these environmental conditions and mechanical excitations, respectively, fatigue loads on wind turbine components also result from grid events, e.g. external power reference signals to actively balance the power flows in the electrical grid. In future power systems with a large proportion of renewable energy sources, the task of conventional power plants to balance the power flow have to be performed mainly by renewable energy power systems. Up to now wind turbines have not been designed to follow an external power reference signal.

So far, some work has been done on this issue and as a result some new control strategies for wind turbines have been proposed. An overview of the difficulties encountered in the implementation of variable power for existing wind turbine control schemes was presented in Aho et al. (2012). A procedure introduced in Erlich and Wilch (2010), Miller and Clark (2010) is the inertial response emulation which provides fast increases (or decreases) in the power production through sudden increases (or decreases) in the generator torque. To maintain a reserve of available wind power the authors in Ma and Chowdhury (2010), Juankorena et al. (2009) propose to operate the turbine at higher than optimal tip-speed ratios. The primary grid response to frequency disturbances in power systems with high penetration of wind turbines being equipped with active power control was considered in de Almeida and Lopes (2007). The results suggesting that active power control (APC) by wind power plants can increase grid robustness and reduce the maximum frequency deviation from nominal during a disturbance.

Due to the described principal advantages that wind power plants with APC functionality can stabilize the electrical grid, the effects of this functionality on the mechanical wind turbine structure must now be investigated. So far, few investigations have been made on this subject. For that reason, model based, nonlinear wind turbine controllers are designed by the Control Engineering Group at HTW Berlin, which also comprise dynamic control by APC for variable power production, e.g. presented in Pöschke et al. (2017), Pöschke et al. (2020). As the dynamic APC func-

tionality is realized by additional actuator activity, additional fatigue loads occur. Therefore, this paper presents the total and overall damage equivalent load as assessment criteria for fatigue loads and applies this criteria on the example on APC of wind turbines.
The paper is organized as follows: First, in Section 2 a non-linear model-based control law for power tracking is described, whereby only the structure is explained here. The focus of Section 3 is on the presentation of an appropriate load assessment criteria for wind turbine control design applied to the example of active power control. This includes the wind turbine simulation model being used, the selection of wind speed profiles and the presentation of load assessment criteria that can be used directly for controller validation in practice. Finally, in Section 4 the simulation results for load analysis with and without power tracking is presented and discussed with regard to the interpretability of the assessment criteria.

2. NON-LINEAR CONTROLLER FOR POWER TRACKING

2.1 Control-oriented wind turbine model

The control-oriented non-linear model of the wind turbine is given in Takagi and Sugeno (1985) (TS) form

$$\dot{x} = \sum_{i=1}^{N_r} h_i(z) \left[A_i(x - x_{0,i}) + B_i(u - u_{0,i}) + B_{d,i}(v - v_{0,i}) \right] \tag{1}$$

with the state vector x, the input vector u, the associated equilibrium points $x_{0,i}$, $u_{0,i}$, and the premise variable vector

$$z = [\, v \,,\, \Delta P \,]^T \,, \tag{2}$$

where v denotes the effective wind speed and ΔP the power tracking signal. The system matrix A_i and inputs matrices B_i and $B_{d,i}$ are obtained by numerical linearisation of the 5MW reference turbine (Jonkman et al. (2009)) using the aero-elastic simulation package FAST (Fatigue, Aeroelastics, Structures and Turbulence) (Jonkman and Buhl Jr. (2005)). In general, TS models like (1) describe non-linear system dynamics as convex combination of linear sub-models where the weighting of each sub-model is determined by the membership function $h_i(z) : \mathbb{R} \to [0, 1]$ that fulfill the convex sum property

$$\sum_{i=1}^{N_r} h_i(z) = 1 \quad \forall z \,. \tag{3}$$

The state vector

$$x = [x_{TW,SS} \,,\, \dot{x}_{TW,SS} \,,\, x_{TW,FA} \,,\, \dot{x}_{TW,FA} \,,\, \omega_r \,,\, \omega_g \,,\, \theta_{DT}]^T \,, \tag{4}$$

of the wind turbine model (1) contains the tower top displacement with $x_{TW,SS}$ as the side-to-side motion, $x_{TW,FA}$ as the fore-aft tower motion, ω_r as the rotor speed, ω_g as the generator speed, and the drivetrain torsion angle θ_{DT}. The control variables of the input vector

$$u = [\, \beta \,,\, T_g \,]^T \tag{5}$$

are the collective pitch angle β and the generator torque T_g. The model-based approach used here requires that the tower top displacement represented by TwSS and TwFA are measurable. With the additional possibility of measuring ω_r and ω_g follows

$$y = C\, x \tag{6}$$

where

$$C = \begin{bmatrix} 1 & 0 & 0 & 0 & 0 & 0 & 0 \\ 0 & 0 & 1 & 0 & 0 & 0 & 0 \\ 0 & 0 & 0 & 0 & 1 & 0 & 0 \\ 0 & 0 & 0 & 0 & 0 & 1 & 0 \end{bmatrix}.$$

2.2 Control law

The control law follows the TS structure of the wind turbine model (1) and consists of a feedback u_{FB} and feedforward term u_{FF}

$$\begin{aligned} u = & \underbrace{- \sum_{i=1}^{N_r} h_i(\hat{v}, \Delta P) K_i(\hat{x} - x_{0,i})}_{u_{FB}} \\ & + \underbrace{\sum_{i=1}^{N_r} h_i(\hat{v}, \Delta P)\, u_{0,i}}_{u_{FF}} \end{aligned} \tag{7}$$

with the feedback gains K_i, the estimated state vector $\hat{x}$ and estimated effective wind speed $\hat{v}$. Both are reconstructed by the following state and disturbance observer.

2.3 State and Disturbance Observer

The state and disturbance observer reconstruct the state vector augmented by the wind speed velocity v defined by

$$\xi = [\, x^T \,,\, v \,]^T \,. \tag{8}$$

Accordingly, the model (1) is augmented by an inflow dynamic of the effective wind speed in front of the rotor plane

$$\dot{v} = -\frac{1}{\tau_v}(v - v_{0,i}) \,. \tag{9}$$

This procedure is based on the approach presented in Gauterin et al. (2015) and Georg (2015). The time constant of the first-order wind model is determined by $\tau_v = 4$ s. Note that the choice of τ_v takes into account the time scale that is relevant for the interaction between rotor dynamics and inflow wind field. The state and disturbance observer is given as

$$\dot{\hat{\xi}} = \sum_{i=1}^{N_r} h_i(\hat{v}, \Delta P) \left[\tilde{A}_i(\hat{\xi} - \hat{\xi}_{0,i}) + \tilde{B}_i(u - u_{0,i}) + L_i(y - \hat{y}) \right] \tag{10}$$

with $\hat{\xi} = [\, \hat{x}^T \,,\, \hat{v} \,]^T$ and $\hat{y} = C\, \hat{x}$ where L_i denotes the observer gain, $\tilde{A}_i$ denotes the augmented system matrix and $\tilde{B}_i$ represents the augmented input matrix.

3. DESIGN OF SIMULATION STUDIES

3.1 Wind Turbine Simulation Model

The simulations are performed with FAST using the wind turbine model mentioned in Section 2. It was chosen as a wind turbine reference model for all simulations in Section 4. FAST is an established tool for wind turbine load

simulations in academia as well as industry. It features multi-degrees of freedom and incorporates the AeroDyn module Laino and Hansen (2002), that considers several aerodynamic effects, important for a very realistic modeling of the energy conversion process in the rotor plane. Further, to analysis the mechanical loads under turbulent wind conditions, the software TurbSim has been used in this paper to generate turbulent wind time series. These time series used in FAST simulation satisfies the requirements of *wind class 1A* and *normal turbulence model A* specified by IEC61400-1 (2005) standard.

3.2 Design Load Cases

To calculate occurring fatigue loads resulting from typical wind turbine operation conditions, the following, representing and recommended Design Load Case (DLC) 1.1 for normal design situations under normal external conditions without any fault conditions according industrial standards (i.e. IEC 61400-1) has been used. DLC 1.1 is a stochastic and turbulent design load case respectively according the *normal turbulence model* to obtain fatigue and ultimate loads in this particular case, for reason of controller limits in lower windspeed regions with mean wind speeds from $\bar{v} = 9$ m/s to $\bar{v} = 25$ m/s in 1 m/s steps with a simulation time of $T = 600$ s.
The active power control mode to provide ancillary service for frequency control of the grid often results in additional excitation of the mechanical structure of the wind turbine. That impact of active power control variation on the mechanical structure caused by external power guiding is analysed under turbulent wind conditions. For quantification of the influence of power guiding, the sinusoidal reference signal illustrated in Figure 3 is used:

$$P_{r,d} = P_r\,(1 - \Delta P)\,, \quad \Delta P = \frac{3\sin(2\pi f_r\, t)}{4} \quad \text{for} \quad f_r = \{\,0.05\,,\,0.1\,,\,0.15\,,\,0.2\,\}\,, \tag{11}$$

where P_r denotes the non reduced rotor power. The influence of active power tracking using (11) is investigated in Section 4.

3.3 Load Assessment Criteria

Assumptions In order to determine an appropriate assessment criterion, two load types have to be distinguished:

(1) Ultimate loads generally quasi-static loads resulting from singular events like deterministic gusts
(2) Dynamic loads resulting from turbulent wind time series that lead to fatigue loads

Within this paper just fatigue loads are taken into account. Additionally, the nominal stress approach is utilized instead of the structural stress approach. The latter comprises complex component stress analysis, which cannot be implemented in a model-based controller design algorithm. The fatigue damage of components results from the occurring load cycles and ranges

$$\begin{aligned}\Delta S &= |S_{max}| - |S_{min}| \\ &= (|S_{min}| + 2\ S_a) - |S_{min}| = 2\ S_a,\end{aligned} \tag{12}$$

where $S_a = S_{max} - S_{mean}$ denotes the load amplitude depending on the static mean load S_{mean}, i.e. $S_a = S_a(S_{mean})$. That means the fatigue damage is caused by

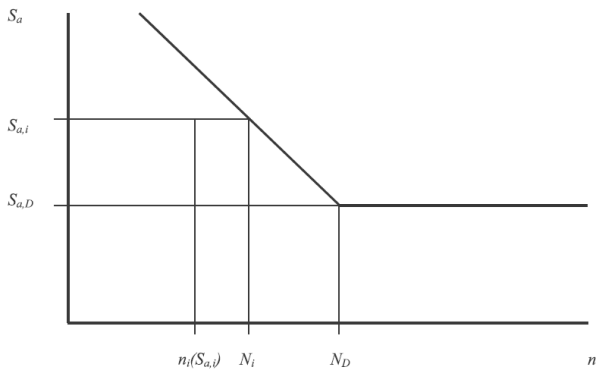

Fig. 1. Example Wöhler Curve

the recurrence of maximum loads S_{max} resulting from load amplitudes S_a oscillating about the mean loads S_{mean}. As mean loads do not only result from occurring external loads, but also result from structural loading, e.g. from the manufacturing process like welding stresses, a precise determination of the mean values is hardly feasible within a control-engineering assessment of a system. Therefore the mean values are neglected within the present work i.e. $S_{mean} = 0$ is assumed. Within this study, the occurring half- and full-cycles with four equal half-cycles or two equal full-cycles forming one load cycle ΔS are identified by a Rainflow-Count algorithm proposed by Niesłony (2010). The fatigue strength and endurable fatigue loads, respectively are described by a Wöhler curve, typically comprising the endurable load amplitudes S_a versus endurable numbers of load amplitudes $N = N(S_a)$ for constant mean loads S_{mean}

$$S_a = \left(\frac{N_D}{N}\right)^{1/k} S_{aD}\,, \tag{13}$$

where k denotes the material depending slope of the S/N-curve, S_{aD} denotes the limiting load amplitude with $N_D = N_D(S_{aD})$ as the related number of amplitudes. For the S/N-slope k the following values taken from Hansen (2008) are specified

- steel parts (tower, machine frame): $k = 4$
- glass-fibre-reinforced-plastics parts (rotor-blades, nacelle): $k = 10$

In the present work, influences on the fatigue strength like the components shape, size, surface roughness and environmental aspects are neglected. So only the material influence, comprised by the slope k, is taken into account. Correspondingly, in the present work it is not necessary to calculate stresses from forces and moments gained from the WT simulations. Instead, calculated forces and moments are taken as criteria for the load assessment.

Damage Equivalent Load (DEL) Amplitudes The load cycles (12) are evaluated at representative parts of the wind turbine root section of the rotor-blade and bottom of lowest tower section. The partial damage D_i caused by n_i recurrences of a constant load cycle ΔS_i is defined by

$$D_i := \frac{n_i}{N_i} \tag{14}$$

where N_i denotes the endurable load cycle number of the ith load cycle amplitude $S_{a,i}(= \Delta S_i/2)$. According to Palmgren and Miner (1945) accumulated linearly to achieve the total damage $D|_{v_j} = D_j$ (resulting from the jth (mean) wind speed time series)

$$D_{\overline{v}_j} = \sum_i D_i\big|_{v_j} \leq 1. \tag{15}$$

The component failure occurs, if the overall damage D (taking the Rayleigh distribution $p(\overline{v}_j)$ of the considered wind time series into account)

$$D = \sum_j p(\overline{v}_j) D_{\overline{v}_j} = \sum_j p(\overline{v}_j) \sum_i D_i\big|_{v_j} \tag{16}$$

exceeds the value one, which represents an overall accumulated partial damage of 100%. From the total damage $D_{\overline{v}_j}$, resulting from the turbulent wind time series v_j with wind speeds $v_j(t)$ oscillating about the mean wind speed $\overline{v}_j$, the total DEL amplitude $S_{a,eq,\overline{v}_j}$ is deduced as a scalar assessment criterion in the following. $S_{a,eq,\overline{v}_j}$ depends only on k, which represents according to (13) the negative slope of the S/N-curve. The damage equivalent load $S_{a,eq,\overline{v}_j}$, which is a constant amplitude cycle for each of the j mean wind speed time series, represents exactly the same damage as that caused by the ith load cycles of the same times series. Hence, the DEL is deduced from the equality of the accumulated, total damage D_{eq} and the equivalent damage $D_{eq,\overline{v}_j}$ of the jth wind time series (where $D_{eq,\overline{v}_j} = \frac{n_{eq,\overline{v}_j}}{N_{eq,\overline{v}_j}}$). With the endurable load cycle number according to (13) (with $N \equiv N_{\overline{v}_j}$ or $N \equiv N_{eq,\overline{v}_j}$) the DEL amplitude results in:

$$\sum_i D_i\big|_{v_j} \stackrel{!}{=} D_{eq,\overline{v}_j} \Leftrightarrow$$

$$S_{a,eq,\overline{v}_j} = \left(\frac{1}{n_{eq,\overline{v}_j}} \sum_i \left(S_{a,i}\big|_{\overline{v}_j} \right)^k \right)^{1/k}, \tag{17}$$

where $S_{a,i}\big|_{\overline{v}_j}$ represents the single load amplitude cycle identified by the Rainflow-Count (RC) algorithm of time series related to the jth mean wind speed $\overline{v}_j$. For the equivalent load cycle number $n_{eq,\overline{v}_j}$ the $\overline{v}_j$ depending, counted load cycle number occuring in $T = 600$ s simulation for the jth mean wind speed $\overline{v}_j$ is determined by RC algorithm. Finally, the overall damage equivalent load $S_{a,eq}$ is given by the accumulated equivalent loads $S_{a,eq,\overline{v}_j}$ of all j mean wind speed time series comprising the complete wind turbine operating time as

$$\sum_j p(\overline{v}_j) D_{eq,\overline{v}_j} = D_{eq} \Leftrightarrow$$

$$S_{a,eq} = \left(\frac{1}{n_{eq}} \sum_j p(\overline{v}_j)\ L_F\ n_{eq,\overline{v}_j}\ S^k_{a,eq,\overline{v}_j} \right)^{1/k} \tag{18}$$

with

$$n_{eq} = \sum_j n_{eq,\overline{v}_j}\ p(\overline{v}_j)\ L_F\ ,$$

where $p(\cdot)$ denotes the Rayleigh distribution function according to the wind speed and class. L_F indicates the total life time factor with respect to the time length of the simulation and assumed life time.
The total damage equivalent load amplitude $S_{a,eq}$ (18) is applied as an load assessment criterion for the tower base fore-aft moment (TwrBsMyt), tower base side-to-side moment (TwrBsMxt), flapwise moment (RootMyb1) and edge wise moment (RootMxb1) of Blade 1 as representative components of the wind turbine structure. The related tower and blade coordinates are shown in Figure 2.

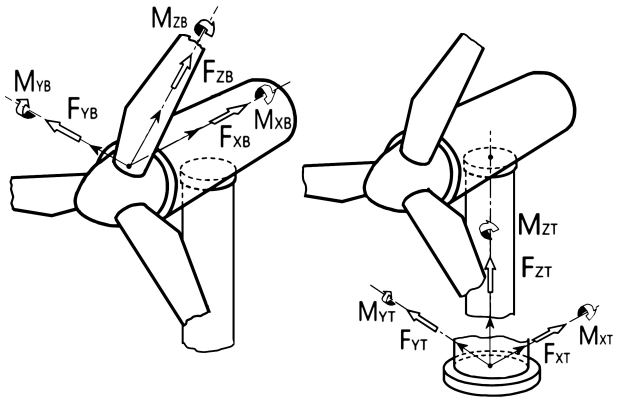

Fig. 2. left: Blade coordinate system with internal torques; right: Tower coordinate system of tower base fore-aft moment and side-to-side moment

4. SIMULATION STUDIES IN POWER TRACKING OPERATION

4.1 System Dynamics of Closed-loop Power Tracking

Before the analysis of fatigue loads the upper dynamic limits of the power tracking control with (7), (10) are to be investigated. For this purpose, we look at the transfer characteristics in the time domain

$$P_r(t) = \mathcal{F}(P_{r,d}(t))|_{\bar{v},\omega_{r,n}} \tag{19}$$

for a given mean wind speed $\bar{v} = 15$ m/s at the nominal rotor speed $\omega_{r,n} = 1.27$ rad/s shown in Figure 3. Here it can be seen that the APC of the 5 MW FAST wind turbine can follow the power reference (11) up to $f_r = 0.2$ Hz. At frequencies above 0.2 Hz, the phase shift increases and the amplitude decreases significantly. Hence, the active power controller performance works up to this frequency. The effects of APC on tower-for-aft moment at this turbulent mean wind speed are illustrated in Figure 4.

4.2 Assessment of the calculated DEL for selected load cases

The fatigue loads resulting from the TS controller (7), (10) without and with APC capability are analysed using the proposed DEL amplitudes $S_{a,eq,\overline{v}_j}$ and $S_{a,eq}$ as assessment criterion:

- First, the fatigue load mitigation potential of a TS controller is recognizable from the comparison of the TS controller without APC to an conventional PI controller (based on the NREL PI controller specification Jonkman and Buhl Jr. (2005)). As illustrated in Figure 5, 7, 9 and 11 the total DEL amplitudes $S_{a,eq,j}$

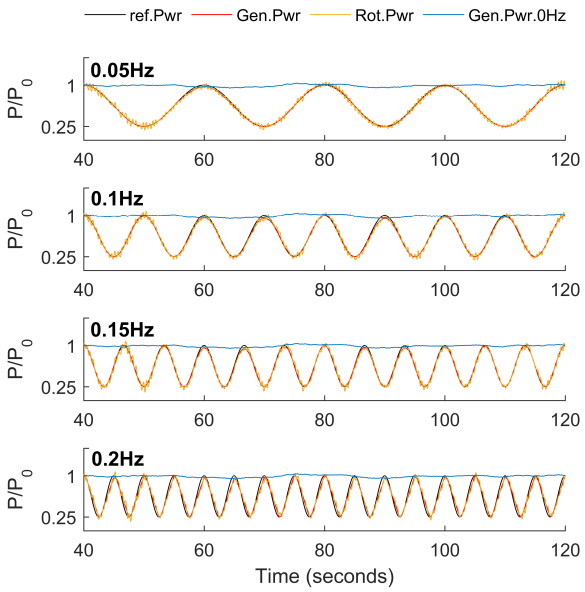

Fig. 3. Control dynamics of the APC wind turbine with respect to the power output (generator power P_g and rotor power P_r) for a sinusoidal reference signal $P_{r,d}$ (ref. rotor power) determined by (11)

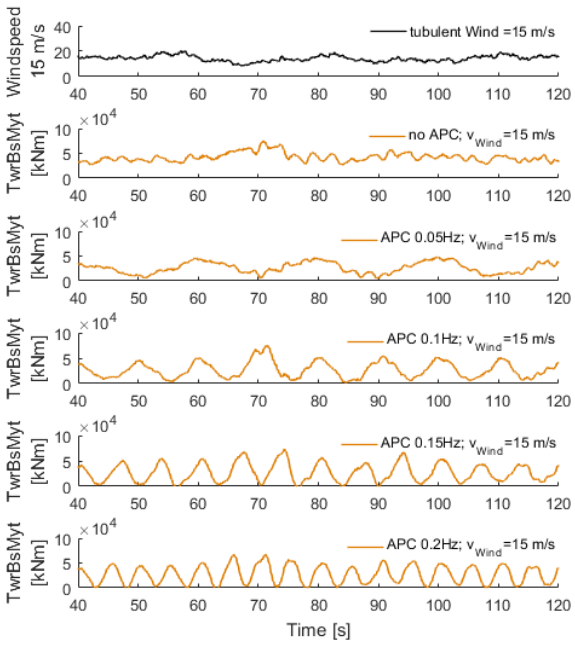

Fig. 4. Dynamics of tower-for-aft moment TwrBsMyt at turbulent windspeed of 15 m/s for given APC cases

resulting from the TS controller are lower – for nearly all wind time series – than those resulting from the PI controller (compare PI with TS for $f = 0$ Hz in the figures mentioned above). Therefore, with consideration of the wind distribution $p(\overline{v}_j)$ the overall DEL amplitude $S_{a,eq}$ is decreased significantly by the TS controller operation (see Figure 6, 8, 10 and 12).

- Second, the fatigue loads resulting from APC are considered. Note that a conventional wind turbine PI controller usually does not provide an APC capability. Therefore, the TS control law with APC cannot be compared with an conventional PI wind turbine controller. But with the DEL amplitude assessment criterion, also taking the wind distribution $p(\overline{v}_j)$ for a more realistic WT load analysis into account, the increase in fatigue load resulting from the APC operation is reasonable. In Figure 5 and Figure 7 the total DEL amplitudes $S_{a,eq,\overline{v}_j}$ of tower base bending moments *TwrBsMxt/ TwrBsMyt* and in Figure 9 and Figure 11 the DEL amplitude $S_{a,eq,\overline{v}_j}$ of blade root bending moments *RootMxb1/ RootMyb1* related to the coordinate system shown in Figure 2 are presented. The selected load case of the turbulent wind time series $\overline{v}_j$ clearly shows the significant influence of the APC operation on the fatigue loads. Note that the external power reference signal with increasing frequency leads to an increasing load. Although this type of sinusoidal power variation will not occur in practice, it shows very clearly the impact of the APC on the fatigue loads.

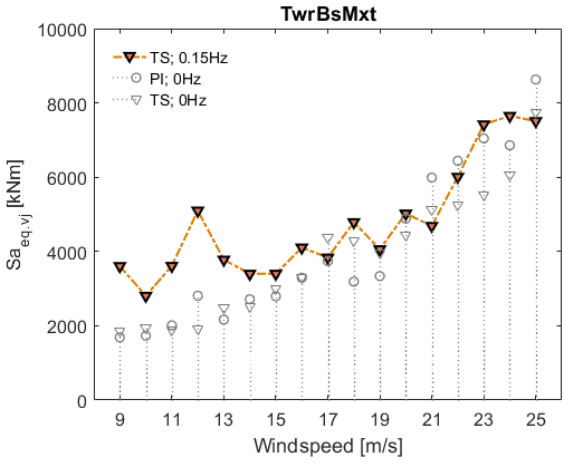

Fig. 5. $S_{a,eq,\overline{v}_j}$ related to tower base side-to-side moment TwrBsMxt for power reference frequency $f_r = 0.15$ Hz with variable mean wind speed $\bar{v}$

5. CONCLUSION

An domain-specific assessment criteria based on Damage Equivalent Loads (DEL) are proposed to quantify the influence of wind turbine control system on fatigue loads of the mechanical main components, the tower and blades. Here the overall DEL amplitudes also take the wind distribution and rainflow counted occurring number of load cycles into account.
To illustrate the practicability of the approach it was used for the assessment of an model-based active power controller (APC). It could be shown that the APC of wind turbines for grid support results in additional loads and thus a reduction of the life cycle. Using the selection of turbulent load cases and their analysis, one can see that even a model-based well-designed control scheme cannot fully compensate the additional loads. But based on the assessment criteria and the quantification of these

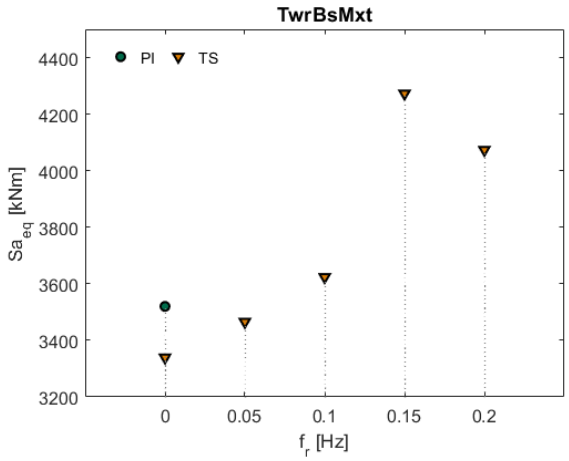

Fig. 6. $S_{a,eq}$ related to tower base side-to-side moment TwrBsMxt with variable power reference frequency f_r determined by (11)

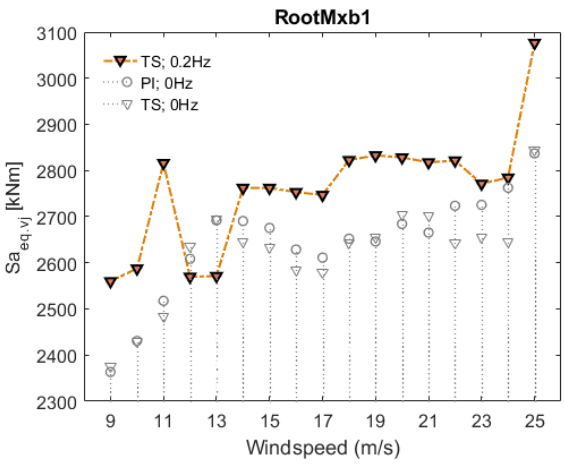

Fig. 9. $S_{a,eq,\bar{v}_j}$ related to edge wise moment RootMxb1 of Blade 1 for power reference frequency $f_r = 0.2$ Hz with variable mean wind speed $\bar{v}$

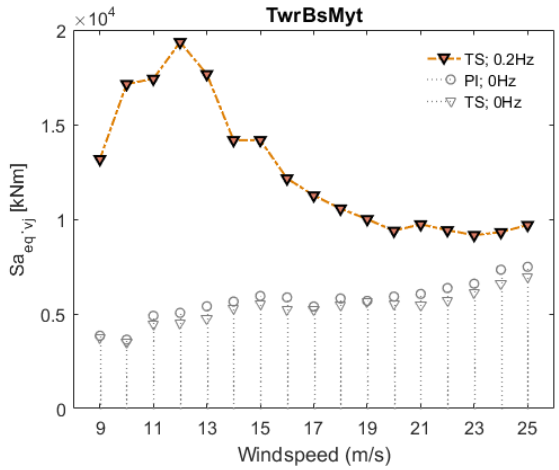

Fig. 7. $S_{a,eq,\bar{v}_j}$ related to tower fore-aft moment TwrBsMyt for power reference frequency $f_r = 0.2$ Hz with variable mean wind speed $\bar{v}$

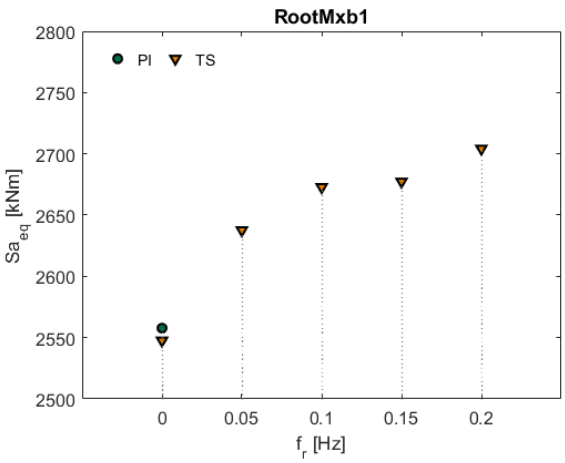

Fig. 10. $S_{a,eq}$ related to edge wise moment RootMxb1 with variable power reference frequency f_r determined by (11)

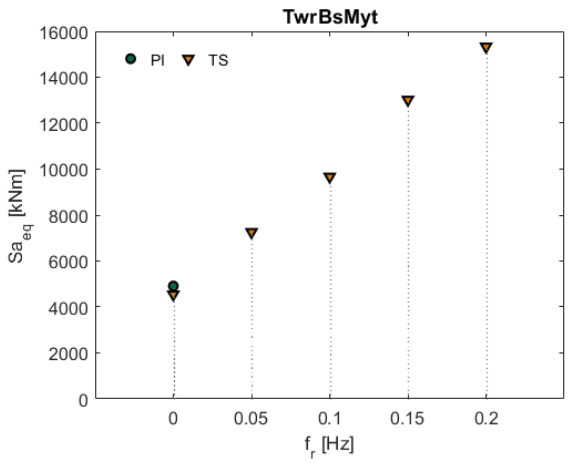

Fig. 8. $S_{a,eq}$ related to tower fore-aft moment TwrBsMyt with variable power reference frequency f_r determined by (11)

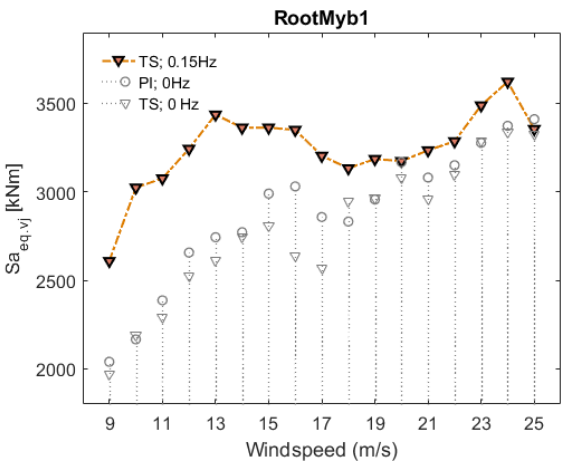

Fig. 11. $S_{a,eq,\bar{v}_j}$ related to flapwise moment RootMyb1 of Blade 1 for power reference frequency $f_r = 0.15$ Hz with variable mean wind speed $\bar{v}$

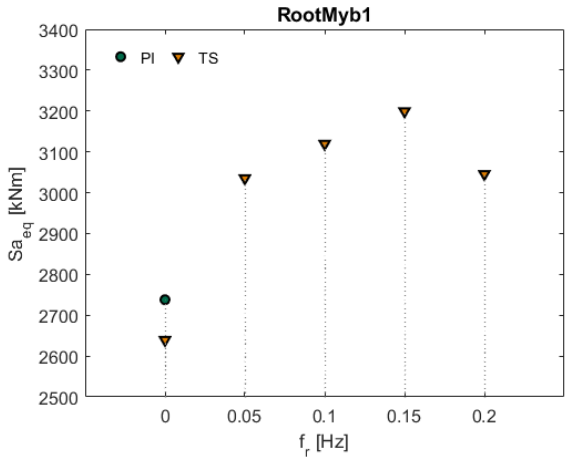

Fig. 12. $S_{a,eq}$ related to flapwise moment RootMyb1 with variable power reference frequency f_r determined by (11)

additional loads, better tailored control systems for wind power plants can be developed.

REFERENCES

Aho, J., Buckspan, A., Laks, J., Fleming, P., Jeong, Y., Dunne, F., Churchfield, M., Pao, L., and Johnson, K. (2012). A tutorial of wind turbine control for supporting grid frequency through active power control. In *2012 American Control Conference (ACC)*.

de Almeida, R. and Lopes, J.P. (2007). Participation of doubly fed induction wind generators in system frequency regulation. *IEEE Transactions on Power Systems*, 22, 944–950.

DNV-GL (2016). Loads and site conditions for wind turbines. Standard, Det Norske Veritas - Germanischer Lloyd SE.

Erlich, I. and Wilch, M. (2010). Primary frequency control by wind turbines. In *IEEE Power and Energy Society General Meeting*.

Gauterin, E., Kammerer, P., Kühn, M., and Schulte, H. (2015). Effective wind speed estimation: Comparison between Kalman Filter and Takagi-Sugeno Observer techniques. *ISA-Transactions*. doi: 10.1016/j.isatra.2015.11.016.

Georg, S. (2015). *Fault diagnosis and fault-tolerant control of wind turbines nonlinear Takagi-Sugeno and sliding mode techniques*. Ph.D. thesis, University Rostock, Fakultät für Maschinenbau und Schiffstechnik.

Hansen, M.O. (2008). *Aerodynamics of Wind Turbines*. Earthscan, 2nd edition.

IEC61400-1 (2005). Wind Turbines (Part 1: Design requirements). Standard, International Electrotechnical Commission.

Jonkman, J., Butterfield, S., Musial, W., and Scott, G. (2009). Definition of a 5-MW Reference Wind Turbine for Offshore System Development. Technical report, NREL/TP-500-38060, National Renewable Energy Laboratory, Golden, Colorado.

Jonkman, J.M. and Buhl Jr., M.L. (2005). FAST User's Guide. Technical report, NREL/EL-500-38230, National Renewable Energy Laboratory, Golden, Colorado.

Juankorena, X., Esandi, I., Lopez, J., and Marroyo, L. (2009). Method to enable variable speed wind turbine primary regulation. In *International Conference on Power Engineering, Energy and Electrical Drives*, 495–500.

Laino, D.J. and Hansen, A.C. (2002). User's Guide to the Wind Turbine Aerodynamics Computer Software AeroDyn. Technical report, Windward Engineering LC, Prepared for the National Renewable Energy Laboratory under Subcontract No. TCX-9-29209-01.

Lendek, Z., Guerra, T.M., Babuška, R., and De Schutter, B. (2010). *Stability Analysis and Nonlinear Observer Design Using Takagi-Sugeno Fuzzy Models*. Springer-Verlag Berlin Heidelberg.

Ma, H. and Chowdhury, B. (2010). Working towards frequency regulation with wind plants: Combined control approaches. *Renewable Power Generation, IET*, 4(4), 308–316.

Miller, N.W. and Clark, K. (2010). Advanced controls enable wind plants to provide ancillary services. In *IEEE Power and Energy Society General Meeting*.

Miner, M.A. (1945). Cumulative damage in fatigue. *Journal of Applied Mechanics*, 12, 159–164.

Niesłony, A. (2010). Rainflow counting algorithm. Technical report. (Set of functions with user guide for use with MATLAB. Download: http://www.mathworks.com/matlabcentral/ fileexchange/3026S).

Pöschke, F., Gauterin, E., Kühn, M., Fortmann, J., and Schulte, H. (2020). Load mitigation and power tracking capability for wind turbines using linear matrix inequality-based control design. *Wind Energy*. doi: 10.1002/we.2516.

Pöschke, F., Fortmann, J., and Schulte, H. (2017). Nonlinear wind turbine controller for variable power generation in full load region. In *American Control Conference (ACC), 20178*, 1395–1400. IEEE, Seattle, WA, USA. doi:10.23919/ACC.2017.7963148.

Takagi, T. and Sugeno, M. (1985). Fuzzy Identification of Systems and Its Application to Modeling and Control. *IEEE Transactions on Systems, Man, and Cybernetics*, 15(1), 116–132.